JOURNAL OF THERMOPHYSICS AND HEAT TRANSFER
Vol. 24, No. 2, April–June 2010

Analysis of Entropy Generation and Thermal Stability in a Slab

A. Aziz*
Gonzaga University, Spokane, Washington 99268
and
O. D. Makinde†
Cape Peninsula University of Technology, Bellville 7535, South Africa

DOI: 10.2514/1.45723

This study investigates the inherent irreversibility in a rectangular slab with temperature-dependent internal heating. It is assumed that the slab external surfaces are subjected to asymmetric heat exchange with the surrounding medium. The simplified governing equation for energy balance in Cartesian coordinates is solved analytically and expedites to obtain expressions for the temperature field, thermal stability criterion, volumetric entropy generation number, and irreversibility distribution ratio. Graphical results are presented and discussed quantitatively. It is found that the local and total entropy generation rates in the slab can be minimized for certain combinations of the heat transfer parameters.

Nomenclature

a	=	temperature dependency of heat generation parameter
Bi_1	=	slab left face Biot number
Bi_2	=	slab right face Biot number
H	=	the slab area
h_1	=	slab left face heat transfer coefficient
h_2	=	slab right face heat transfer coefficient
k	=	constant thermal conductivity
L	=	half-thickness of the solid slab
Q	=	internal heat generation parameter
$\dot{q}_r$	=	reference heat generation
$\dot{S}'''$	=	volumetric rate of entropy generation
T	=	temperature
T_r	=	reference temperature
T_1	=	slab left face temperature
T_2	=	slab right face temperature
X	=	nondimensional coordinate
x	=	Cartesian coordinate
α	=	heat generation constant
θ	=	nondimensional temperature
λ	=	temperature asymmetry parameter
Ω	=	temperature difference parameter

I. Introduction

THE problem of heat conduction in a solid slab with internal heat generation is of fundamental importance in many engineering applications. These include heat transfer gauges, thermal insulations, metal casting, ice formation, thermal control of space vehicles, etc. [1,2]. For instance, the reduction of structural damage caused by aerodynamic heating in space vehicles has been given an increasing amount of attention. To protect space vehicles, a variety of design methods have been used in practice; these include the use of heat sinks, transpiration cooling, and mass-transfer cooling.

Moreover, the elementary analysis of one-dimensional steady-state conduction in a slab with constant and uniform internal heat generation can be found in many heat transfer textbooks [3,4]. The temperature distribution in a slab for the more general case of temperature-dependent internal heat generation has been presented by Gebhart [5]. He also discussed the criterion that must be met to avoid thermal instability, which may lead to thermal destruction of the slab due to excessively high temperatures. Cheung et al. [6] investigated the problem of one-dimensional heat conduction within a finite slab that was subjected to a realistic laser pulse profile. It was found that both surface convection and material properties affect the peak temperature location within the slab over time. Their results provide an improved model of laser heating at a surface by combining a spatially and temporally decaying laser pulse with a finite slab. The optimum dimension and heat conduction in an extended surface operating in a convective environment was investigated by Aziz [7].

Moreover, it is now widely recognized that heat transfer problems that were previously studied using the first law of thermodynamics can be reexamined in the light of the second law of thermodynamics, so that thermal systems can be designed with the objective of minimizing thermodynamic irreversibility. This design methodology, known as entropy generation minimization, is comprehensively covered in Bejan [8]. One theoretically correct measure of thermodynamic performance is the magnitude of thermodynamic irreversibility associated with a component or process. It can be shown that the minimization of entropy generation also results in the maximum reduction of irreversibility. The development of improved thermal designs is enhanced by the ability to identify clearly the source and location of entropy generation. Many studies have been published to assess the sources of irreversibility in components and systems. Khan et al. [9] analyzed the minimization of the entropy generation of a tube bank in cross flow. Ibanez et al. [10] investigated the unsteady entropy generation rate due to an instantaneous internal heat generation in a solid slab. Their results revealed that a direct relationship exists between the basic heat transfer mechanics: heat conduction, heat convection, and internal heat generation. Other applications of second law analysis can be found in [11–14].

The objective of this study is to investigate the heat conduction process and entropy generation in an asymmetrically cooled, one-dimensional slab experiencing internal heat generation that is a linear function of temperature. The thermal stability criterion is discussed. Results for the temperature distribution, location of maximum temperature, local rate of entropy generation, and total entropy generated in the slab are presented, illustrating the effects of heat generation parameters, a temperature difference parameter, and the Biot

Received 29 May 2009; revision received 13 August 2009; accepted for publication 15 August 2009.

*Department of Mechanical Engineering, School of Engineering and Applied Science; aziz@gonzaga.edu.
†Faculty of Engineering, Post Office Box 1906; makinded@cput.ac.za.

numbers characterizing the convection processes on the two faces of the slab. In the following sections, the problem is formulated, analyzed, and solved. The results are presented graphically and discussed quantitatively.

II. Energy Analysis

Consider a one-dimensional slab of thickness L made of a material with uniform and constant thermal conductivity k (see Fig. 1).

The slab is experiencing internal heat generation, which is a linear function of temperature, that is,

$$\dot{q} = \dot{q}_r[1 + \alpha(T - T_r)] \tag{1}$$

where $\dot{q}_r$ is the heat generation at reference temperature T_r, and α is a constant. The left face ($x = 0$) is cooled by a convection process characterized by the coolant temperature T_1 and heat transfer coefficient h_1. The right face of the slab is cooled by a convection process characterized by the coolant temperature T_2 and heat transfer coefficient h_2. Assuming uniform thermophysical properties, the one-dimensional steady heat conduction equation governing the system is

$$\frac{\mathrm{d}^2T}{\mathrm{d}x^2} + \frac{\dot{q}}{k} = 0 \tag{2}$$

and the corresponding boundary conditions are

$$k\frac{\mathrm{d}T}{\mathrm{d}x}(x = 0) = h_1[T(x = 0) - T_1] \tag{3}$$

$$k\frac{\mathrm{d}T}{\mathrm{d}x}(x = L) = -h_2[T(x = L) - T_2] \tag{4}$$

The problem can be rendered dimensionless by defining

$$\theta = \frac{T - T_r}{T_1 - T_r}, \qquad X = x/L, \qquad Bi_1 = \frac{h_1 L}{k}, \qquad Bi_2 = \frac{h_2 L}{k}$$
$$\lambda = \frac{T_2 - T_r}{T_1 - T_r}, \qquad Q = \frac{\dot{q}_r L^2}{k(T_1 - T_r)}, \qquad a = \alpha(T_1 - T_r) \tag{5}$$

Substituting Eq. (5) into Eqs. (2–4), we obtain

$$\frac{\mathrm{d}^2\theta}{\mathrm{d}X^2} + Q(1 + a\theta) = 0 \tag{6}$$

with

$$\frac{\mathrm{d}\theta}{\mathrm{d}X} = Bi_1(\theta - 1), \quad \text{at } X = 0 \tag{7}$$

$$\frac{\mathrm{d}\theta}{\mathrm{d}X} = -Bi_2(\theta - \lambda), \quad \text{at } X = 1 \tag{8}$$

It is evident that θ is a function of X, Q, a, Bi_1, λ, and Bi_2. It would be particularly interesting to study how the location of maximum temperature in the slab is affected by parameters Q, a, Bi_1, λ, and Bi_2.

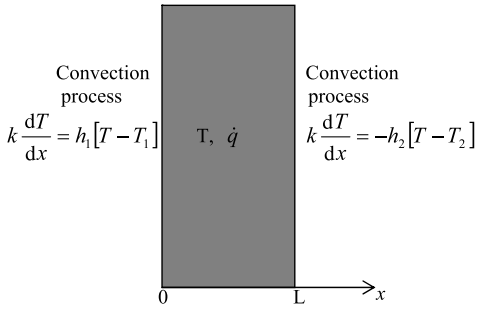

Fig. 1 Sketch of the physical model.

Equation (6) is a simple second-order linear nonhomogenous ordinary differential equation. Its exact solution is given as

$$\theta(X; Q > 0, a > 0) = -(1/a) + A\sin(X\sqrt{Qa}) + B\cos(X\sqrt{Qa}) \tag{9}$$

where A and B are constants to be determined from the boundary conditions in Eqs. (7) and (8). Using a computer algebra package like MAPLE [15], the values of A and B can be easily obtained as

$$\begin{aligned} A = {} & (Bi_1(Bi_2 + Bi_2\lambda a - Bi_2\cos(\sqrt{Qa}) - Bi_2\cos(\sqrt{Qa})a \\ & + \sin(\sqrt{Qa})\sqrt{Qa} + \sin(\sqrt{Qa})\sqrt{Qa}a))/ \\ & (a(\cos(\sqrt{Qa})\sqrt{Qa}Bi_1 + Bi_2\sin(\sqrt{Qa})Bi_1 \\ & + \sqrt{Qa}Bi_2\cos(\sqrt{Qa}) - \sin(\sqrt{Qa})Qa)) \end{aligned} \tag{10}$$

$$\begin{aligned} B = {} & (\sqrt{Qa}Bi_2 + \sqrt{Qa}Bi_2\lambda a + \cos(\sqrt{Qa})\sqrt{Qa}Bi_1 \\ & + Bi_2\sin(\sqrt{Qa})Bi_1 + \cos(\sqrt{Qa})\sqrt{Qa}aBi_1 \\ & + Bi_2\sin(\sqrt{Qa})aBi_1)/(a(\cos(\sqrt{Qa})\sqrt{Qa}Bi_1 \\ & + Bi_2\sin(\sqrt{Qa})Bi_1 + \sqrt{Qa}Bi_2\cos(\sqrt{Qa}) \\ & - \sin(\sqrt{Qa})Qa)) \end{aligned} \tag{11}$$

It is important to note that the temperature field solution in Eqs. (9–11) is only valid for $a > 0$ and $Q > 0$. However, when $a = 0$ the problem corresponds to the case of constant internal heat generation and Eq. (6) then reduces to $\mathrm{d}^2\theta/\mathrm{d}X^2 = -Q$; its solution with respect to the boundary conditions in Eqs. (7) and (8) becomes

$$\begin{aligned} \theta(X; Q > 0, a = 0) = {} & -\frac{1}{2}QX^2 \\ & + \frac{1}{2}\frac{Bi_1(2Q + 2Bi_2\lambda + Bi_2Q + 2Bi_2)X}{Bi_1 + Bi_2 + Bi_2Bi_1} \\ & + \frac{1}{2}\frac{2Q + 2Bi_1 + 2Bi_2\lambda + 2Bi_2Bi_1 + Bi_2Q}{Bi_1 + Bi_2 + Bi_2Bi_1} \end{aligned} \tag{12}$$

When $Q = 0$, the solution in Eq. (12) reduces to that of the temperature field in a slab without internal heat generation and is given by

$$\begin{aligned} \theta(X, Q = 0) = {} & \frac{1}{2}\frac{Bi_1(2Bi_2\lambda - 2Bi_2)X}{Bi_1 + Bi_2 + Bi_2Bi_1} \\ & + \frac{1}{2}\frac{2Bi_1 + 2Bi_2\lambda + 2Bi_2Bi_1}{Bi_1 + Bi_2 + Bi_2Bi_1} \end{aligned} \tag{13}$$

The location of maximum temperature in the slab can be obtained by differentiating Eqs. (9–13) with respect to X and setting the derivative to zero.

III. Thermal Stability Criterion

The solution for the temperature field in the slab becomes infinite if the denominator is zero [5]. Examination of the denominator of Eq. (9) reveals that a finite solution exists if the following conditions are met:

$$\text{If } aQ = Bi_1Bi_2, \quad \text{then } \sqrt{aQ} \neq (2n + 1)\pi/2n \quad \text{for integer } n \tag{14}$$

$$\text{If } aQ \neq Bi_1Bi_2, \quad \text{then } \tan\sqrt{aQ} \neq \frac{(Bi_1 + Bi_2)\sqrt{aQ}}{Qa - Bi_1Bi_2} \tag{15}$$

Conditions (14) and (15) indicate that the thermal stability of the slab depends not only on the heat generation parameters but also on the thickness of the slab and its thermal conductivity, as well as the parameters characterizing the convection processes. Moreover, it is

interesting to note that the thermal stability of the slab without internal heat generation or with constant internal heat generation, as highlighted in Eqs. (12) and (13), depends only on the asymmetric convective cooling parameters and is given by $Bi_1 + Bi_2 \neq -Bi_1 Bi_2$.

IV. Entropy Analysis

The study of entropy generation in conductive and convective heat transfer processes has assumed considerable importance since the pioneering work of Bejan [8]. Since then, numerous papers have studied entropy generation in heat transfer processes, of which [9–14] are a representative sample. On the other hand, studies of entropy generation in pure conduction processes have been very limited. It was therefore felt important to perform such calculations for the present problem. The volumetric rate of entropy generation $\dot{S}'''$ at any location in a slab with internal heat generation is given by [10]

$$\dot{S}''' = \frac{k\left(\frac{dT}{dx}\right)^2}{T_r^2} + \frac{\dot{q}}{T_r} \tag{16}$$

which may be integrated over the slab thickness to give the total entropy generated in the slab as follows [4]

$$\dot{S} = \int_0^L \dot{S}''' H \, dx \tag{17}$$

where H is the slab area normal to the heat flow direction. Equations (16) and (17) are expressed in dimensionless form as

$$Ns = \frac{L^2 T_r^2 \dot{S}'''}{k(T_1 - T_r)^2} = \left(\frac{d\theta}{dX}\right)^2 + \frac{Q}{\Omega}(1 + a\theta) \tag{18}$$

$$N_T = \int_0^1 Ns \, dX \tag{19}$$

where $\Omega = (T_1 - T_r)/T_r$ is the temperature difference parameter. In Eq. (18), the first term due to temperature gradient can be assigned as N_1 and the second term due to internal heat generation as N_2, that is,

$$N_1 = \left(\frac{d\theta}{dX}\right)^2, \qquad N_2 = \frac{Q}{\Omega}(1 + a\theta) \tag{20}$$

To have an idea whether internal heat generation dominates over heat transfer irreversibility or vice versa, we define the irreversibility distribution ratio as $\Phi = N_1/N_2$. Internal heat generation dominates for $0 \leq \Phi < 1$ and heat transfer dominates when $\Phi > 1$. The contribution of both heat transfer and internal heat generation to entropy production are equal when $\Phi = 1$.

V. Results and Discussion

In this section, the numerical results for various physically relevant values of the embedded parameters controlling the thermal system under investigation are presented in Tables 1 and 2 and graphically in Figs. 2–5. These results validate the analytical expression obtained earlier in Secs. II, III, and IV.

A. Maximum Temperature Location

From a practical perspective, the knowledge of how the location of the maximum temperature is affected by the various parameters is important. It provides a better understanding of heat treatment manufacturing processes in microtechnology and space vehicle equipments, for which precise control of the location of the maximum temperature is required. This information for X is provided in Table 1 for a fixed value of $Bi_2 = 1$ and for various combination values of parameters a, λ, Q, and Bi_1. The last column shows that X increases with an increase in each of the parameters a, λ, Q, and Bi_1. Table 2 provides the data for X, illustrating the effect of variation of Bi_2 for $a = 0.1$, $\lambda = 0.1$, $Q = 1$, and $Bi_1 = \infty$. The value of $Bi_1 = \infty$ implies that the left face of the slab is at the temperature of its surrounding coolant. As Bi_2 increases, X decreases, which means the location of the maximum temperature moves closer to the left face of the slab.

Table 1 Computations showing the values of X at which $\frac{d\theta}{dX} = 0$ for different parameter values ($Bi_2 = 1$)

a	λ	Q	Bi_1	X
0.1	0.1	1.0	1.0	0.23138
0.5	0.1	1.0	1.0	0.32944
0.7	0.1	1.0	1.0	0.36729
1.0	0.1	1.0	1.0	0.41502
0.1	1.0	1.0	1.0	0.50000
0.1	1.5	1.0	1.0	0.64019
0.1	2.0	1.0	1.0	0.77378
0.1	0.1	2.0	1.0	0.37313
0.1	0.1	3.0	1.0	0.42053
0.1	0.1	5.0	1.0	0.45858
0.1	0.1	1.0	2.0	0.27556
0.1	0.1	1.0	10	0.32520
0.1	0.1	1.0	100	0.33893
0.1	0.1	1.0	∞	0.34052

Table 2 Computations showing the values of X at which $\frac{d\theta}{dX} = 0$ ($a = 0.1$, $\lambda = 0.1$, $Q = 1$, $Bi_1 = \infty$)

Bi_2	X
0.1	0.88325
0.2	0.78460
0.3	0.70029
0.4	0.62751
0.5	0.56410
0.6	0.50841
0.7	0.45914
0.8	0.41526
0.9	0.37594
1.0	0.34052
2.0	0.11606
3.0	0.00420

B. Effect of Various Parameters on Temperature Distribution

The effect of parameter a on the temperature distribution in the slab is shown in Fig. 2a for identical Biot numbers on the two sides of the slab, that is, $Bi_1 = Bi_2 = 1$, and the temperature asymmetry parameter $\lambda = 0.1$. The value of $\lambda = 0.1$ indicates that the temperature of the coolant on the right side of the slab is much lower than the temperature of the coolant on the left side of the slab. Consequently, more heat is dissipated from the right face of the slab, as can be seen from larger temperature gradients at $X = 1$. The parameter a is a measure of the strength of temperature dependency of heat generation. For $a = 0$, the internal heat generation in the slab is constant and a low slab temperature is observed. As a increases, the temperature in the slab gets elevated throughout and the location of the maximum temperature in the slab gradually shifts toward the midpoint of the slab ($X = 0.5$). Figure 2b illustrates how the temperature asymmetry parameter λ affects the temperature distribution in the slab for $Bi_1 = Bi_2 = 1$, $a = 0.1$, and $Q = 1$. The slab temperature increases in an increasing value of λ. As λ increases from 0.1 to 2, the temperature of the coolant on the right side of the slab increases to a much higher level than the temperature of the coolant on the left side of the slab and the location of the maximum temperature shifts toward the right face of the slab. In Fig. 2c, the effect of internal heat generation on the temperature profiles in the slab is illustrated for $Bi_1 = Bi_2 = 1$, $a = 0.1$, and $\lambda = 0.1$. When

$Q = 0$, no internal heat generation is present and a low slab temperature is observed. As Q increases, the heat generation becomes more intense and causes the temperature in the slab to increase. Because T_2 is much lower than T_1, a larger portion of the heat leaves the right face of the slab, as indicated by the larger temperature gradients at $X = 1$. Figure 2d displays the temperature profiles in the slab for increasing values of Bi_1, with other parameters fixed at $a = 0.1$, $\lambda = 0.1$, $Bi_2 = 1$, and $Q = 1$. As expected, the effect of increasing Bi_1 (i.e., increasing the heat transfer coefficient h_1) is to lower the temperature levels throughout the slab. Despite the fact that h_1 is equal to or greater than h_2, the heat dissipation from the right face is larger than that from the left face because T_2 is much lower than T_1 in view of $\lambda = 0.1$. Furthermore, the results in Figs. 2a–2d are in agreement with the ones reported in [6,10,11].

C. Effect of Various Parameters on Local Entropy Generation Rate

Figure 3a shows the local entropy generation rate for increasing values of Bi_1, with the remaining parameters fixed at the values indicated in the figure caption. The entropy generation is low at the left face and high at the right face. The bulk of entropy generation occurs in the right half of the slab because of the larger temperature gradients created as a result of T_2 being much lower than T_1 and the higher heat dissipation from the right face, as reported in Fig. 2d. The minimum entropy generation decreases as Bi_1 increases. The minimum entropy generation occurs between $X = 0.2$ and 0.4, depending on the value of Bi_1. The local entropy generation rate for increasing values of Q is shown in Fig. 3b. The entropy generation rate steadily increases as one proceeds from the left face of the slab to its right face. As the intensity of heat generation increases, that is, Q increases, the entropy generation rate also increases. The effect of temperature asymmetry parameter λ on the entropy generation rate is illustrated in Fig. 3c. Each curve shows that the entropy generation rate decreases as X increases, reaches a minimum, and then increases. The location of the minimum entropy generation rate shifts toward the right face of the slab with an increasing value of λ. The curves tend to overlap in the region $X = 0.4$ and 0.8. Figure 3d illustrates the effect of temperature-dependent internal heat parameter a on the local entropy generation rate. The entropy generation rate increases as a increases. The entropy generation rate gradually decreases, reaching a minimum value at some distance away from the left face of the slab, and then increases toward the right face of the slab.

D. Effect of Various Parameters on Total Entropy Generated

The total entropy generated in the slab is plotted in Fig. 4a for different values of parameter a. In each case the total entropy generated initially decreases as Bi_1 increases and later approaches an asymptotic value. As a increases, the total entropy generated in the slab gets elevated throughout. Figure 4b illustrates the effect of asymmetric convective cooling on the total entropy generated in the slab. For $Bi_2 = 1$ and 2, the total entropy generated initially decreases as Bi_1 increases but exhibits asymptotic behavior, as in Fig. 4a. However, for $Bi_2 = 5$ and 10, the pattern is reversed. The entropy generated increases as Bi_1 increases but the curves do manifest asymptotic behavior. Moreover, it is noteworthy that, for certain combinations of thermal parameters, the total entropy generated in the slab with asymmetrical cooling is minimized. A similar conclusion was reached by Ibanez et al. [10] for viscous flow between parallel plates with asymmetric convective cooling at the plate. The curves in Fig. 4c, which delineate the effect of coolant temperature asymmetry, exhibit an interesting pattern for $\lambda = 1$, 1.5, and 2.0. For these values, the total entropy generated initially decreases as Bi_1 increases, reaches a minimum value, and then increases to reach an asymptotic value. As λ increases, the total generated in the slab increases. Figure 4d shows the effect of parameter Q on the total entropy generation. For $Q = 0.1$ and 0.5, the total entropy generated increases as Bi_1 increases but rapidly approaches an asymptotic value. However, for $Q = 0.7$ and 1, the total entropy generated decreases as Bi_1 increases and reaches an asymptotic value quickly.

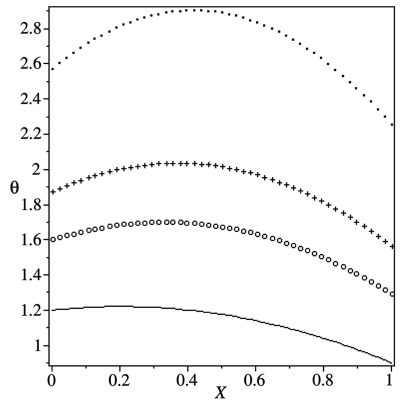

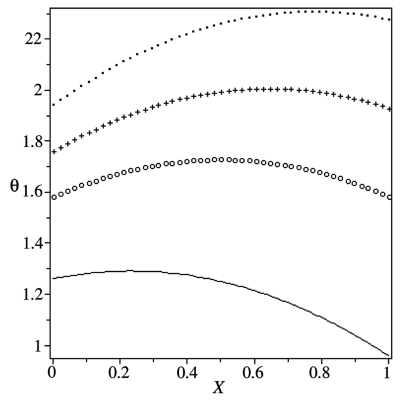

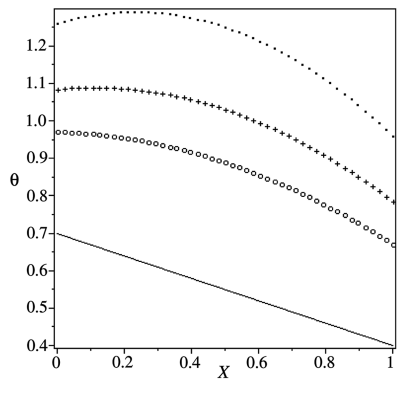

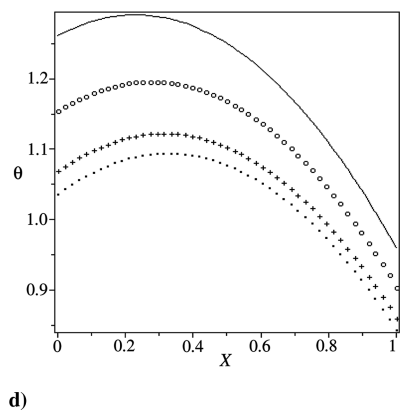

Fig. 2 Temperature profile: a) $Bi_1 = 1$; $Bi_2 = 1$; $\lambda = 0.1$; $Q = 1$; line: $a = 0$; circles: $a = 0.5$; plus signs: $a = 0.7$; dots: $a = 1$. b) $Bi_1 = 1$; $Bi_2 = 1$; $a = 0.1$; $Q = 1$; line: $\lambda = 0.1$; circles: $\lambda = 1$; plus signs: $\lambda = 1.5$; dots: $\lambda = 2$. c) $Bi_1 = 1$; $Bi_2 = 1$; $a = 0.1$; $\lambda = 0.1$; line: $Q = 0$; circles: $Q = 0.5$; plus signs: $Q = 0.7$; dots: $Q = 1$. d) $Q = 1$; $Bi_2 = 1$; $a = 0.1$; $\lambda = 0.1$; line: $Bi_1 = 1$; circles: $Bi_1 = 2$ plus signs: $Bi_1 = 5$; dots: $Bi_1 = 10$.

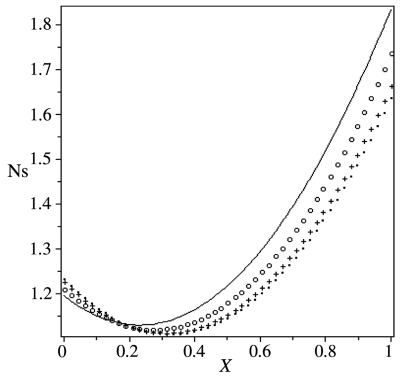

a)

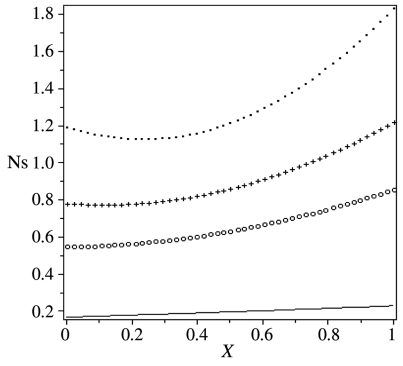

b)

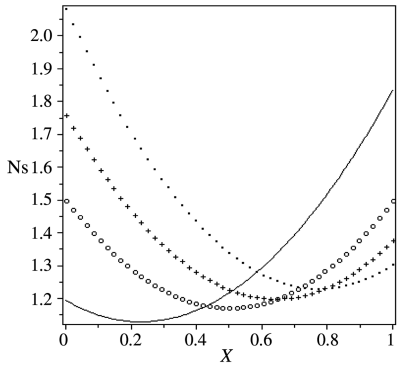

c)

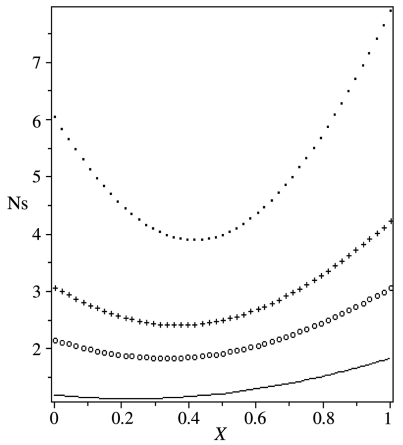

d)

Fig. 3 Entropy generation rate: a) $\Omega = 1$; $Q = 1$; $Bi_2 = 1$; $a = 0.1$; $\lambda = 0.1$; line: $Bi_1 = 1$; circles: $Bi_1 = 2$; plus signs: $Bi_1 = 5$; dots: $Bi_1 = 10$. b) $\Omega = 1$; $Bi_1 = 1$; $Bi_2 = 1$; $a = 0.1$; $\lambda = 0.1$; line: $Q = 1$; circles: $Q = 0.5$; plus signs: $Q = 0.7$; dots: $Q = 1$. c) $\Omega = 1$; $Bi_1 = 1$; $Bi_2 = 1$; $a = 0.1$; $Q = 1$; line: $\lambda = 0.1$; circles: $\lambda = 1$; plus signs: $\lambda = 1.5$; dots: $\lambda = 2$. d) $\Omega = 1$; $Bi_1 = 1$; $Bi_2 = 1$; $\lambda = 0.1$; $Q = 1$; line: $a = 0.1$; circles: $a = 0.5$; plus signs: $a = 0.7$; dots: $a = 1$.

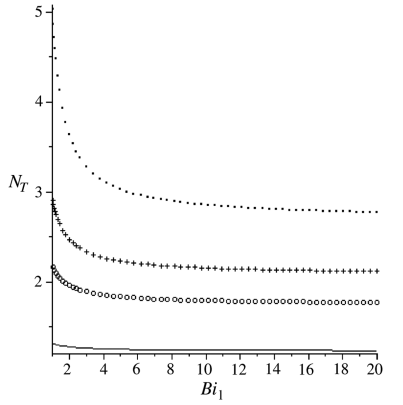

a)

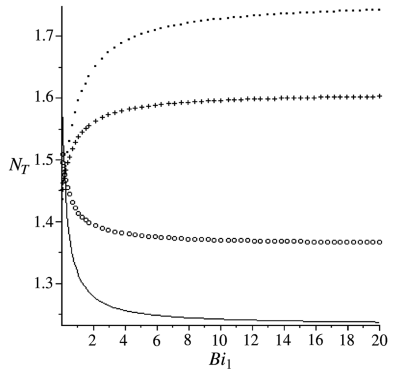

b)

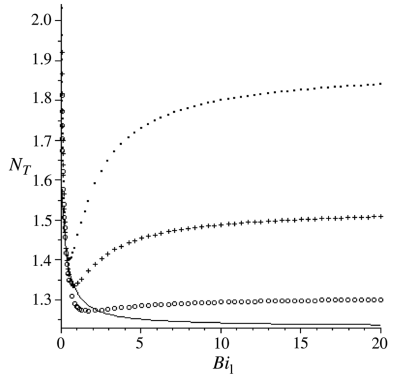

c)

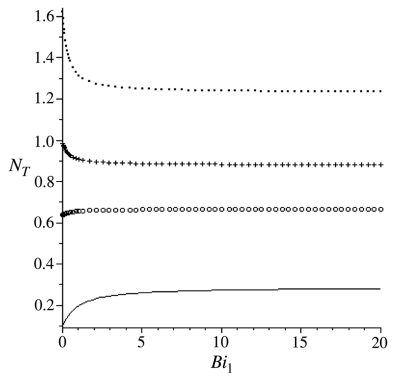

d)

Fig. 4 Total entropy generation: a) $\Omega = 1$; $Bi_2 = 1$; $\lambda = 0.1$; $Q = 1$; line: $a = 0.1$; circles: $a = 0.5$; plus signs: $a = 0.7$; dots: $a = 1$. b) $\Omega = 1$; $Q = 1$; $a = 0.1$; $\lambda = 0.1$; line: $Bi_2 = 1$; circles: $Bi_2 = 2$; plus signs: $Bi_2 = 5$; dots: $Bi_2 = 10$. c) $\Omega = 1$; $Bi_2 = 1$; $a = 0.1$; $Q = 1$; line: $\lambda = 0.1$; circles: $\lambda = 1$; plus signs: $\lambda = 1.5$; dots: $\lambda = 2$. d) $\Omega = 1$; $Bi_2 = 1$; $a = 0.1$; $\lambda = 0.1$; line: $Q = 0.1$; circles: $Q = 0.5$; plus signs: $Q = 0.7$; dots: $Q = 1$.

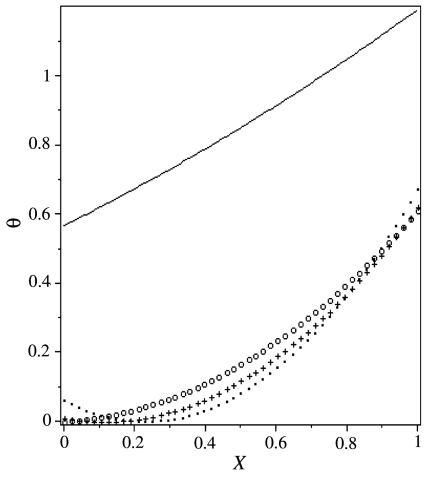

a)

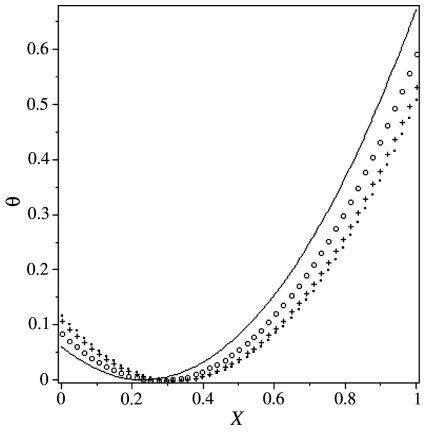

b)

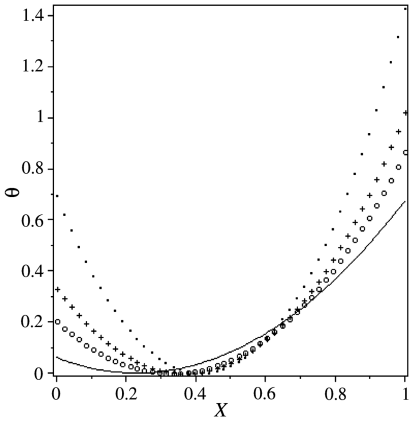

c)

Fig. 5 Irreversibility ratio: a) $\Omega = 1$; $Bi_2 = 2$; $a = 0.1$; $\lambda = 0.1$; line: $Q = 0.1$; circles: $Q = 0.5$; plus signs: $Q = 0.7$; dots: $Q = 1$. b) $\Omega = 1$; $Q = 1$; $Bi_2 = 1$; $a = 0.1$; $\lambda = 0.1$; line: $Bi_1 = 1$; circles: $Bi_1 = 2$; plus signs: $Bi_1 = 5$; dots $Bi_1 = 10$. c) $\Omega = 1$; $Bi_1 = 1$; $Bi_2 = 1$; $\lambda = 0.1$; $Q = 1$; line: $a = 0.1$; circles: $a = 0.5$; plus signs: $a = 0.7$; dots: $a = 1$.

E. Effect of Various Parameters on the Irreversibility Distribution Ratio

The irreversibility distribution ratio between the entropy generated by the temperature gradient and the internal heat generation across the slab is displayed in Figs. 5a–5c. It is interesting to note that internal heat generation irreversibility dominates almost the entire slab. However, the dominant effect of internal heat generation irreversibility is more pronounced towards the left face of the slab. The dominant effect of heat transfer irreversibility is only apparent at the right face of the slab with decreasing values of Q and increasing values of parameters a and Bi_1.

VI. Conclusions

The evaluation of the entropy production rates in a slab with asymmetric convective cooling and temperature-dependent internal heat generation was carried out analytically. Closed-form analytical solutions were obtained for the temperature field and the thermal stability criterion. The volumetric entropy generation rate and irreversibility ratio depend on the Biot number (Bi_1, Bi_2), temperature asymmetry parameter (λ), internal heat generation parameters (Q), temperature-dependent internal heat parameter (a), and the slab thickness (X). Our results reveal that the entropy generation rate in the slab increases with an increase in parametric values of Q, a, and λ. The internal heat generation irreversibility dominates almost the entire slab. However, both the local and total entropy generation rates in the slab can be minimized for certain combinations of the heat transfer parameters. Finally, the geometrical configuration of many heat conducting materials used in many engineering systems such as space vehicles may be approximated with a solid slab, in so far as their heat transfer characteristics are concerned. The performance and optimum design of this material is enhanced by the ability to identify clearly the source and location of entropy generation for minimization purpose. In addition, the present paper considers asymmetric convective boundary conditions at the two faces of the slab and develops a new thermal stability criterion that is not available elsewhere. Our results will no doubt be of engineering interest.

Acknowledgments

The authors gratefully acknowledge the valuable suggestions of the anonymous referees. Author Makinde would also like to thank the National Research Foundation of South Africa Thuthuka program for financial support.

References

[1] Incropera, F. P., and DeWitt, D. P., *Fundamentals of Heat and Mass Transfer*, Wiley, New York, 1996.

[2] Bakos, G. C., "Direct Heat Generation and Corresponding Energy Saving in Nuclear Reactors Due to Optimum Synthesis of Shielding Materials," *Annals of Nuclear Energy*, Vol. 29, 2002, pp. 1381–1387. doi:10.1016/S0306-4549(01)00121-9

[3] Ozisik, M. N., *Heat Conduction*, 2nd ed., Wiley, New York, 1993.

[4] Arpaci, V. S., and Larsen, P. S., *Convection Heat Transfer*, Prentice–Hall, 1984, p. 39.

[5] Gebhart, B., *Heat Conduction and Mass Diffusion*, McGraw–Hill, New York, 1993.

[6] Cheung, T. K., Blake, B. A., and Lam, T. T., "Heating of Finite Slabs Subjected to Laser Pulse Irradiation and Convective Cooling," *Journal of Thermophysics and Heat Transfer*, Vol. 21, No. 2, 2007, pp. 323–329. doi:10.2514/1.23100

[7] Aziz, A., "Optimum Dimensions of Extended Surfaces Operating in a Convective Environment," *Applied Mechanics Reviews*, Vol. 45, No. 5, 1992, pp. 155–173. doi:10.1115/1.3119754

[8] Bejan, A., *Entropy Generation Minimization*, CRC Press, Boca Raton, FL, 1996.

[9] Khan, W. A., Culham, J. R., and Yovanovich, M. M., "Optimal Design of Tube Banks in Cross Flow Using Entropy Generation Minimization Method," *Journal of Thermophysics and Heat Transfer*, Vol. 21, No. 2, 2007, pp 372–378. doi:10.2514/1.26824

[10] Ibanez, G., Cuevas, S., and de Haro, M. L., "Minimization of Entropy Generation by Asymmetric Convective Cooling," *International Journal of Heat and Mass Transfer*, Vol. 46, 2003, pp. 1321–1328. doi:10.1016/S0017-9310(02)00420-9

[11] Bautista, O., Méndez, F., and Martinez-Meyer, J. L., "(Bejan's) Early vs. Late Regimes Method Applied to Entropy Generation in One-

Dimensional Conduction," *International Journal of Thermal Sciences*, Vol. 44, 2005, pp. 570–576.
doi:10.1016/j.ijthermalsci.2004.10.006

[12] Aziz, A., "Entropy Generation in Pressure Gradient Assisted Couette Flow with Different Thermal Boundary Conditions," *Entropy*, Vol. 5, 2003, pp. 271–312.
doi:10.3390/e5030271

[13] Rastogi, S. K., and Poulikakos, D., "Second-Law Optimization of Forced Convection of Non-Newtonian Fluids in Ducts," *Journal of Thermophysics and Heat Transfer*, 0887–8722 Vol. 6, No. 3, 1992, pp 540–543.
doi:10.2514/3.394

[14] Makinde, O. D., "Irreversibility Analysis of Variable Viscosity Channel Flow with Convective Cooling at the Walls," *Canadian Journal of Physics*, Vol. 86, No. 2, 2008, pp. 383–389.
doi:10.1139/P07-126

[15] Heck, A., *Introduction to Maple*, 3rd ed., Springer–Verlag, Berlin/New York/Heidelberg, 2003.